# FIELD EMISSION ARRAY CATHODE MATERIAL SELECTION FOR COMPATIBILITY WITH ELECTRIC PROPULSION APPLICATIONS

C. M. Marrese-Reading[1], J. Polk[1], W. A. Mackie[2]
[1]Jet Propulsion Laboratory, Pasadena, CA 91109
[2]Applied Physics Technologies, McMinnville, OR 97128

## ABSTRACT

One of the critical challenges in integrating field emission array cathodes with electric propulsion systems is material. Experimental results from compatibility studies show these environments will detrimentally affect the cathode work function, conductivity, and tip morphology. In the investigation discussed in this paper, the response of FEA cathodes and FEA material candidates to simulated electric propulsion system environments are presented. Materials considered include ZrC/Mo, Mo, MgPt, Pt, NbC/Nb, NbNi/Nb, Nb, RuTa/Ta, Ru/Ta and Ta. The results of the measurements suggest that NbC/Nb, NbNi/Nb, and MgPt are the most promising candidates. The details motivating this conclusion are discussed.

## INTRODUCTION

Field emission (FE) cathodes are under development for electric propulsion systems because of their superiority over thermionic cathodes in power, mass, and expellant consumption. The electric propulsion systems which could benefit from the field emission cathode technology operate at relatively low power levels which are comparable to thermionic cathode power levels. These systems include low power Hall (<200 W), ion (<200 W), colloid (<5 W) and field emission electric propulsion (FEEP) thrusters (<5 W) and electrodynamic tethers. Hall and ion thrusters require the electron source to ionize the propellant and neutralize the ion beam and thruster charge. Colloid and FEEP thrusters require electron sources to neutralize the thruster charge. Electrodynamic tethers (EDT) require the electron source to drive the electrons out of the tether and through the ionospheric plasma.

Field emission cathodes have already demonstrated compatibility with colloid thrusters and indium-FEEPs. Although the compatibility experiments conducted were only preliminary because of their short durations, the results were remarkably promising. The Mo field emission array (FEA) cathode from SRI International improved the performance of the thruster by >50% with respect to the performance with a state-of-the-art thermionic cathode. This experiment was conducted at a thruster operating point of ~8 μN and 66 μA , which is near to the target operating point for the Laser Interferometry Space Antenna (LISA) mission. Thruster charge neutralization has also been demonstrated with a colloid thruster and carbon nanotube cathode. [1]

Other electric propulsion systems require more advanced field emission cathode configurations and materials for compatibility because of their hostile environments, voltage limitations, and current densities required. EDTs will require 10-20 mA/cm$^2$ in a low Earth orbit environment, which is predominantly atomic oxygen at $10^{-7}$ Torr. Field emission cathode materials traditionally used are very sensitive to oxygen. This environment affects the cathode performance with work function and conductivity changes. Experimental results have shown that limited exposure to oxygen during operation produces reversible cathode performance changes. The cathode performance is not affected by the same exposures with the cathode not operating. Prolonged exposure to oxygen during operation does result in irreversible performance changes. Oxygen ionized locally can contribute to tip blunting from ion bombardment if the ion energies exceed the energy threshold for sputtering. Experimental results suggest that this operating voltage limitation exceeds 60 V. For this application, a FEA cathode material is required which is compatible with the cathode fabrication process, has low work function and forms a conductive and low work function oxide in atomic oxygen. The work function required depends on the cathode geometry, fabrication uniformity, and operating voltage limitations. Many materials have been identified for this application because of their chemical and work function stability in oxidizing environments.

Even more challenging compatibility issues exist with other electric propulsion applications. Small scale ion thrusters which generate a few millinewtons of thrust require cathodes capable of 10-200 mA/cm$^2$ in a highly ionized environment. Because these thrusters primarily operate with xenon propellant, the cathodes must operate in a predominantly xenon environment. The low ionization potential of xenon results in a significant population of xenon ions which can sputter the tip material if their energies exceed the energy threshold for sputtering, which has been estimated to be ~36 eV. Therefore the cathode must be operated so that the energy of self-generated and thruster ions

bombarding the tips does not exceed 36 eV. Because the testing environment of the thrusters is not UHV, the cathode must also be fairly resistant to contamination by background oxygen. Experimental results have shown that FEA cathodes can be operated in xenon environments similar to the thruster environments without permanent performance degradation, however, temporary performance degradation observed may be attributable to contamination by background oxygen. In this case, the cathode under development for the EDT application should also benefit the Hall and ion thruster applications.

This paper includes discussions of the electric propulsion systems and their demands on cathode performance, experimental results from FEA cathode testing in electric propulsion system environments, details from a cathode material candidate selection program, and the current course of our program.

## ELECTRIC PROPULSION SYSTEM APPLICATIONS FOR FEA CATHODES

In this section, the configuration and performance of several meso- and microscale electric thrusters are described, the cathode performance requirements are presented, and the cathode environments are discussed. Mesoscale ion and Hall thrusters have the advantage of higher thrust levels and an inert propellant. Colloid and field emission thrusters have the advantage of scalablility in size and power to be compatible with microscale spacecraft. Many of the mesoscale and microscale thrusters being considered are still under development; the performance of larger systems are discussed in this section with performance objectives for the miniature systems. It is obvious that the performance of each of these systems will be significantly improved with a compatible FE cathode. Tables are presented at the end of the section describing the performance of state-of-the-art systems and the cathode environment.

*Mesoscale ion engines*

An ion engine has three major components as shown in Figure 1: (1) the discharge chamber, (2) the ion optics and (3) a neutralizer cathode. Propellant injected into the discharge chamber is ionized by electron bombardment in a low pressure discharge. Permanent magnets oriented axially near the anode trap the electrons and impede their flow to the anode. The ion optics are composed of two multi-aperture grids which are biased to accelerate and focus ions which drift into the interelectrode gap. The neutralizer cathode produces electrons to neutralize the ion beam positive space charge. Modeling has shown that the ionization efficiency of the discharge chamber is unacceptably low if the device scale is too small, primarily because the higher surface-to-volume ratio results in excessive plasma losses to the walls. Current research is therefore focused on mesoscale thrusters with MEMS components, rather than microfabricated engines.

Ion engines have been optimized and flight qualified to operate at power levels up to 2.3 kW. Mesoscale contact ion thrusters were developed to operate on cesium with considerable success; however, xenon propellant is preferred over cesium because of its toxicity. Cesium ion thrusters have demonstrated 12 μN at 4.58 W from a 1.27 cm-diameter discharge chamber up to 5.3 mN at 237 W from a 4.58 cm-diameter discharge chamber [2]. At low power levels, the thermionic cathode consumed as much as 48 % of the total power consumed by the thruster. More recently, the performance of a xenon ion thruster with a 5 cm-diameter discharge chamber was reported as 2.2 mN and 2300 s at 49% thrust efficiency and 50 W of power [3]. The efficiency calculation does not include the power and propellant consumption by the cathode. The reported performance of the 5-cm thruster is described in Table 1. The development approach currently being implemented relies on a conventional electron bombardment discharge chamber with xenon propellant, field emitter cathodes, conventional chemically-etched metal grids or MEMS grids [4] and a field emitter neutralizer. The mesoscale engines being developed will have discharge chambers 1 to 5 cm in diameter and will operate at power levels of 10 to 300 W. The desired operating characteristics are an exhaust speed of 36 km/s (specific impulse of 3600 s), thrust levels of 0.5 to 5 mN, an efficiency of 50% at 300 W, and lifetimes of up to 6000 hours. NASA GRC thruster information

A FE cathode compatible with an ion thruster could significantly improve the system efficiency. The anticipated requirements on a discharge cathode is emission of up to 1 A (100-200 $mA/cm^2$) reliably over 6000 hours into xenon gas with a pressure of up to $10^{-4}$ torr and a plasma density of $10^{11}/cm^3$. The neutralizer cathode must also operate for over 6000 hours and be capable of emitting up to 40 mA in the environment near the exit plane of the thruster, where xenon gas pressures may be as high as $10^{-5}$ Torr and the charge-exchange ion current densities should be less than 0.004 $mA/cm^2$. The charge-exchange ions will be accelerated through approximately 20 V between the plasma and the cathode gate electrode.

*Mesoscale Hall thrusters*

A Hall thruster is an electrostatic propulsion device which also ionizes the propellant by electron bombardment, like ion thrusters. A cross-section of a Hall thruster is shown in Figure. Propellant is injected through the anode into the

discharge chamber. A single cathode is used to emit electrons which ionize the propellant and neutralize the ion beam. The potential applied between the anode and cathode creates an axial electric field to accelerate the ions. Inner and outer electromagnets create a radial magnetic field with large gradients near the physical exit plane of the thruster. The electrons enter the discharge chamber and become confined by the magnetic field in an azimuthal drift towards the anode. Propellant is ionized in the electron cloud. The ions are primarily accelerated in the discharge chamber by the axial electric field to generate thrust. Because of the high electron density in the ionization and acceleration region, this thruster is capable of providing current densities higher than the ion thruster can generate, and therefore higher thrust densities.

Hall thrusters have been optimized to operate at 1.5 -3.0 kW and are currently being scaled down to mesoscale systems which will be optimized to generate 1-10 mN of thrust. Higher pressures, current densities, and magnetic field strengths are then required to reduce mean free paths in the discharge chamber and maintain the plasma discharge as the size of the thruster is reduced [5]. The X-40 [6], D-32 [7], and a 50 W [5] Hall thruster fall into the mesoscale thruster category. Xenon is the preferred propellant for these systems because of its high mass, relatively low ionization energy, and inert nature. The X-40 has a 40 mm discharge chamber diameter. Its performance was reported as 7.43 mN of thrust at 100 W (150 V, 0.67 A) and 0.74 mg/s to generate 1020 s specific impulse (ion velocities of ~10.2 km/s) at 37 % efficiency (not including the cathode power and propellant). At 200 W and 14.5 mN, the thruster efficiency reported was 48 %. The lifetime of this system was projected to be 850 hours. It might be increased up to 2000-3000 hours by employing more sputter resistant materials. The D-32, with a 32 mm diameter discharge chamber demonstrated 4.3 mN at 75.6 W (120 V, 0.63 A) and 0.6 mg/s at 20 % efficiency. At 172 W (200V, 0.88 A) and 0.9 mg/s, the D-32 operated at 27 % efficiency. The D-32 and X-40 both used electromagnets to facilitate magnetic field optimization at each operating point. Permanent magnets were used in the 50 W thruster developed with a 3.7 mm discharge chamber because of its small size and potentially high operating temperatures of the electromagnets. While medium scale Hall thrusters with 100 mm discharge chamber diameters require magnetic fields of 300 Gauss, the 50 W thruster required magnetic fields exceeding 5000 Gauss. This thruster operated at 100 W (250 V, 0.38 A) and 0.021 mg/s to generate 773 s at 6 % efficiency. The performance of this thruster was limited, in part, by the magnetic system used. The magnetic field configuration could not be optimized at each operating point and the high operating temperature of the thruster could have affected the performance of the magnets. The thrust efficiency also tends to decrease with decreasing discharge chamber diameter.

According to the results received, miniaturization of the Hall thruster seems to be limited to a 40 mm discharge chamber to achieve at least 30 % efficiency. These thrusters were tested with a hollow cathode and the thruster performance described does not consider cathode power and propellant consumption. Consideration of the hollow cathode performance also decreases the efficiency of the system by several percent.

A field emission cathode compatible with a Hall thruster could significantly improve the performance of the mesoscale propulsion systems. The lifetime of an X-40 with improved materials should be 2000-3000 hours, therefore the same cathode lifetime will be required in the cathode environment. The cathode current requirement ranges from 0.1 to 1 A. The cathode current density objective is 100 $mA/cm^2$.

The cathode environment of a Hall thruster consists of xenon neutrals and ions. One of the xenon ion populations near the cathode originates from charge-exchange collisions between ions in the thruster ion beam and ambient neutrals. The xenon pressure near the cathode depends on propellant flow rate, thruster performance, and vacuum chamber pumping speed. During ground testing of an X-40, this pressure should range between $10^{-6}$ and $10^{-5}$ Torr. The charge-exchange collisions produce fast neutrals and slow ions. The slow ions are then accelerated by local electric fields which can direct them towards the cathode. These ions will then bombard the cathode emitting surface after being accelerated through 20 V in addition to the voltage difference between the emitting surface and the gate electrode. The characteristics of these species have not been quantified; however, ion current density, $J_i$, estimates can be made by scaling measurements made on larger systems with discharge current [8,9]. It is estimated that the charge-exchange $J_i$ will be approximately 2.2 $\mu A/cm^2$ at a thruster discharge current of 0.5 A and local pressure of $2x10^{-5}$ Torr, based on current scaling from measurements taken in the environment of a 70 mm Hall thruster [8].

*Meso- and microscale FEEPs and I-LMISs*

Field Emission Electric Propulsion (FEEP) and Indium Liquid Metal Ion Source (I-LMIS, also referred to In-FEEP) systems also accelerate ions electrostatically to generate thrust; however, unlike the ion and Hall thrusters, the propellant is not ionized by electron bombardment; the propellant is field ionized. FEEPs use cesium and I-LMISs use indium liquid metal propellant which is fed by capillary forces from the propellant reservoir through a small channel (FEEP), or wicked up the outside of a needle from the propellant reservoir (I-LMIS). The emitters are terminated with sharp edges and biased positively with respect to an extraction electrode located downstream of the emitter. The Cs-FEEP slit emitter configuration is shown in Figure a, and the In-FEEP configuration is shown in Figure b. The electric

field applied between the electrodes increases the surface charge density which causes a deformation of the surface of the liquid metal into Taylor cones with a cusp (often called a jet) to maintain equilibrium between electrostatic and surface tension forces [10]. The cusps cause geometric field enhancement, which further reduces the radius of curvature of the tip of the cusp, and in turn, further increases the electric field at the tip. When the electric field strength reaches $10^7$ V/cm, atoms of metal on the tip are ionized by field ionization or field evaporation. Liquid metal is converted into an ion beam without the transitional vapor phase. Electrons are collected by the emitter and channel walls and ions are accelerated by the applied electric field through the slit in the extraction electrode which doubles as the acceleration electrode. Cs-FEEPs are typically fabricated with a slit geometry to increase the throughput. The slit width is typically ~1.2 μm. The gap between the channel and extraction electrode is ~1 mm. The applied voltage between the electrodes is typically 9 kV. The thrust can be throttled by adjusting the applied voltage to control the beam energy and ion generation rate.

The performance of this system depends on emitter geometry, electrode configuration, propellant, and applied voltage. Cesium and indium are preferred propellants because they have low ionization potentials, high atomic masses, effectively wet metal surfaces, and offer compact storage on spacecraft as solids. Each system has unique advantages. The lower vapor pressure of indium results in a lower propellant leak rate. The less reactive nature of indium results in a more robust system which does not require special handling on the ground to prevent contamination by the environment. Cesium melts at a lower temperature ($T_{MCs}$=28.4°C and $T_{MIn}$=157°C) than Indium, therefore less heater power is required for the Cs-FEEP. Cesium propellant is easily contaminated. I-LMISs have been used for spacecraft potential control and are now being developed for propulsion applications also [11]. They are being developed to operate at 1-100 μN and 4.5-10 kV, >6000 s specific impulse at ~15 μN/W (67 W/mN) and recently demonstrated 500 hours of continuous operation with no performance degradation. Cesium FEEP systems have been developed to operate at 66 W/mN for 40 μN of thrust at 9000 s specific impulse (~90,000 m/s ion velocities) with 2.7 W of power. Larger Cs-FEEPs have demonstrated 1400 μN at 9000 s and 93 W. The thrust level depends on the emitter (extraction) electrode voltage and slit length. A Cs-FEEP with a 2 mm-slit produces 40 μN with 5.5 kV on the emitter electrode and –5 kV on the acceleration electrode while a 70 mm slit has demonstrated 1.4 mN at the same operating voltages [12].

Miniature field ionization ion sources have been demonstrated with arrays of volcano-shaped ion emitting cones similar to Spindt-type field emitter electron sources [13,14]. Arrays of these gated cones have been microfabricated with 1.5 μm cone heights with 1 μm apertures in the cones and 15 μm apertures in the gate electrodes. They have been fabricated with 106 volcano tips/cm$^2$. The advantage of this configuration is that the thrust and specific impulse could be independently controlled by addressing only segments of the arrays. This thruster configuration will also be more compact and lightweight than the larger systems; therefore it will be more compatible with microscale to picoscale satellites. The challenge with this system is maintaining high propellant utilization. Microscale field ionization electric thrusters are still under development.

FEEPs and I-LMISs require an electron source only for ion beam neutralization. Hollow, thermionic, and filament cathodes have been used with FEEPs. A cesium hollow cathode demonstrated 10 W/mA [**Error! Bookmark not defined.**]. FE cathodes have demonstrated much higher efficiencies in UHV environments, < 1mW/mA. The FEEP cathode is required to deliver up to several milliamperes in the cesium environment. Both Cs ions and neutrals will interact with the cathode to affect its performance. While it has been demonstrated that cesium improves the performance of FE cathodes, it will reduce emission stability. Experimental and theoretical results have shown that the charge-exchange back-flow ion current is 1 % of the beam current [**Error! Bookmark not defined.**]. With a beam current of 0.9 mA, the plasma density was reported to be $2.4 \times 10^8$. The charge-exchange current density to the cathode region was calculated to be 0.2 μA/cm$^2$, and then scaled with beam current for the estimates shown in Table 1. In this system, it has been shown that the energy of singly charged ions bombarding the cathode could be as high as 100 eV [**Error! Bookmark not defined.**]. It is expected that the demands on the cathode performance will be similar for each thruster, with performance requirements defined by Regime II in Table 2.

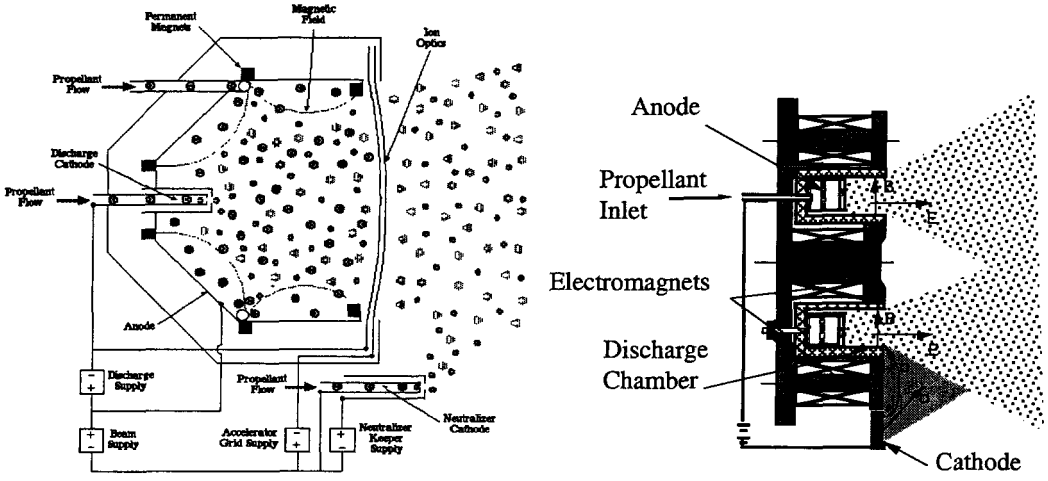


**Figure 1. a) Ion thruster configuration and b) Hall thruster configuration.**

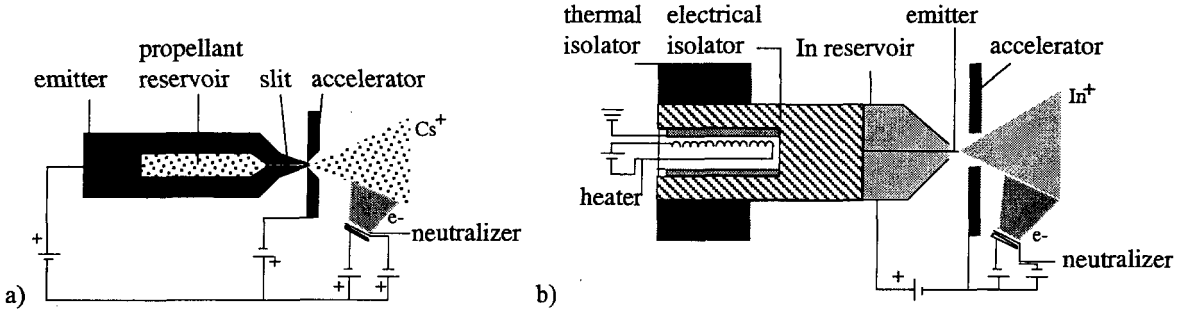


**Figure 2. a) Cs-FEEP slit emitter configuration and b) In-FEEP (I-LMIS) needle emitter configuration.**

## MESO- AND MICROSCALE COLLOID THRUSTERS

Colloid thrusters are similar to FEEPs except that charged droplets, instead of atomic ions are emitted and accelerated [15,16] from the sharp tips of capillary tubes. An electric field is applied between the capillary tubes feeding the propellant and the extraction electrode to increase the surface charge density in the liquid. At the critical surface charge density, the unstable surface forms a cone-jet configuration [17]. Incipient droplets are polarized and ruptured into two portions of net charge [18]. One portion remains at the tip and the other escapes from the fluid and is accelerated by the electric field. The droplets are either positively or negatively charged depending on the propellant used. A bipolar thruster employs both positively and negatively charged droplets [15]. Operating in this mode, the thruster is self-neutralizing. The fluid used in a colloid thruster has a much higher surface tension than the fluid used in FEEPs, primarily generating charged colloids instead of atomic ions. Non-conducting fluids are doped to increase conductivity and colloid emission frequency. A high and uniform specific charge (coulomb per droplet mass) is optimal to maximize the specific charge efficiency and specific impulse. If electric field strengths, fluid conductivity, and propellant flow rates are too high, droplet streams with a large distribution of droplet charge-to-mass ratios (low specific charge efficiency) are created.

The performance of colloid thrusters depends on the propellant, the capillaries, and the applied electric field. High solvation capability, low vapor pressure, low freezing points, and low corrosivity are desired attributes of the propellant. Glycerol is a commonly used propellant. Glycerol doped with sodium iodine produces positively charged droplets. Glycerol doped with sulfuric acid produces negatively charged droplets. Platinum capillaries provide high resistance to corrosion, maximizing thruster lifetime. Bipolar colloid thrusters were developed with platinum capillaries having 200 μm inner diameters using sodium iodide and sulfuric acid doped glycerol propellants. They produced thrust between 0.2 and 0.5 mN at power levels of about 4.4 W/mN, requiring voltages of 4.4 and -5.8 kV, depending on droplet polarity [15]. Specific impulses between 450 and 700 s were estimated. Specific impulses up to 1350 s have also been obtained at 0.55 mN thrust [19]. Current levels are on the order of 10-100 μA.

Colloid thrusters have not yet been miniaturized, but miniaturization is the focus of some research programs.20 These thrusters are natural candidates for miniaturization because the high electric fields required for charged droplet emission can be obtained at reduced voltages with reduced dimensions. However, high accelerating voltages (~10 kV)

will be required to attain a specific impulse near 1000 s. It should be possible to operate these thrusters at milliwatt power levels and integrate them into stacked chip structures for microscale spacecraft.

When a colloid thruster is not operated in bipolar mode and emits only a positive stream of ions, a charge neutralizer will be required. An electron source must be used which operates at power levels comparable with 4.4 W/mN thruster performance. Filament and hollow cathodes operate at higher powers than this thruster at the required current levels of approximately 0.1 mA. A thermionic cathode will operate at a power level comparable to the thruster (0.5 mN at 2.2W with the cathode power approximately 1.5 W). A field emission cathode could easily provide the 0.1 mA required at much lower power levels, however, the cathode must tolerate the thruster environment with minimal effect on performance for > 4000 hours. The colloid thruster will generate a fairly hostile environment as colloids may be deposited on the cathode. The pressure in the cathode region and ion flux to the cathode depend on the vacuum chamber pressure and performance of the thruster. This environment has not yet been characterized

**Table 1. Representative performance and cathode environment of meso- and microscale propulsion systems.**

| | **Mesoscale Ion Thruster (5 cm)[3]** | **Mesoscale Hall Thruster (X-40)[6]** | **Mesoscale FEEP Thruster [12,Error! Bookmark not defined.]** | **Mesoscale Colloid Thruster[15]** |
|---|---|---|---|---|
| Thrust (mN) | 2.2-4.7 | 5-32 | 0.0001-2 | 0.2-0.5 |
| Power (W) | 50-116 | 80-510 | 2.7-93 | 0.88-2.2 |
| Power/Thrust | 23 | 16 | 66 | 4.4 |
| Specific Impulse (s) | 2,300-3,100 | 1,160-1,933 | 6000-11000 | 450-700 |
| Current (mA) | 230-430 (discharge)<br>44-81 (neutralizer) | 500-1,700 | 0.25 (0.05 mN)<br>0.5 (0.1 mN) | - |
| Efficiency | 0.49-0.61 | 0.31-0.55 | 0.98 | 0.50-0.78 |
| Thruster Specific Mass (kg/W) | - | - | 0.008 | - |
| Propellant | Xenon | Xenon | Cesium | Glycerol |
| $J_i(\mu A/cm^2)$ | 4,000 (discharge)21<br>0.004-0.008 (neutralizer) | 2 -7 | 0.002-2 | - |
| Pressure (Torr) | $10^{-3}$-$10^{-6}$ | $10^{-6}$-$10^{-4}$ | $10^{-6}$ | - |
| Lifetime (hours) | 6,000 | 950 (demonstrated),<br>2000 (anticipated) | 450-20,000 | 4,300 |

## INTEGRATION CHALLENGES

The primary concerns with integrating FE cathodes with EP systems are space-charge limited emission and cathode lifetime in the plasma environments generated by the propulsion systems. Typically FE cathodes are operated in a close-spaced triode or diode configuration with one electrode as the anode. In an EP system the FE cathodes will have to operate in a diode configuration with a gate electrode and the local plasma providing a virtual anode. The space-charge current limit depends on the plasma density and temperatures, and electron beam energy and current density. This process has been modeled for some scenarios showing that ~125 mA/cm$^2$ should be the upper current density limit in a Hall thruster environment with 30 eV electron energies.[22]

The lifetime is reduced by erosion and contamination processes and sudden arcing events or shorting by debris. The cathode performance is exponentially sensitive to changes in tip work function and geometry. It is also sensitive to changes in conductivity of the surface induced by oxidation. The cathode lifetime will be limited, through performance degradation, because it will be subjected to constant ion bombardment which can sputter the sharp tips if the energy of the ions exceeds the energy threshold for sputtering. The self-generated ion population originates near the cathode when the electrons emitted by the cathode ionize ambient neutrals. The second ion population of charge-exchange (CEX) ions is generated near the thruster. This ion-rich environment can cause permanent changes in the structure of the emitting surface and temporary changes in the cathode work function, severely affecting the cathode performance because the performance of these cathodes is exponentially sensitive to the radius of curvature and work function of the tips. Because the cathodes will not be operating in UHV facilities with most of the thrusters, the cathodes will be subjected to higher levels of contamination which can affect the cathode work function, conductivity, and frequency of arcing events. Thruster current requirements and environment characteristics are shown in Table 1. The flux of ions to the cathode expected is given as $J_i$. It is clear that there are two regimes that define the cathode performance required. These two regimes are shown in Table 2. Ideally, one cathode will be developed that satisfies both regime I and regime II.

**Table 2. FE cathode performance requirements for two thruster current regimes.**

| Regime | Current Density ($mA/cm^2$) | Gate Voltage (V) | Current/Power (mW/mA) | Lifetime (hours) |
|---|---|---|---|---|
| I | 50-200 | ≤36 | ≤10 | >6,000 |
| II | 1-10 | ≤20-100 | ≤10 | 450-20,000 |

## APPROACH TO INTEGRATION

For FE cathodes to be compatible with EP systems, they must meet the current density and lifetime requirements in their environments. While their power and propellant efficiencies are much higher than conventional cathode technologies, they must also meet the lifetime requirements and consume less than 10 mW/mA through the gate electrode. The performance objectives for FE cathodes compatible with mesoscale and microscale electric propulsion systems are described in Table 2. There are two performance regimes targeted. Regime I represents the cathode performance required by the propulsion systems generating millinewton thrust levels and requiring hundreds of milliamperes of current. Regime II represents the cathode performance required by the propulsion systems generating micronewton thrust levels and requiring tens to hundreds of microamperes of current. An efficiency of at least 10 mW/mA will be required to satisfy the power limitations of picosatellites with less than 100 mW total power. The tolerable power consumption of the gate electrodes will further limit the cathode efficiency. The values in Table 3 represent the demands on the cathodes by the electric propulsion systems only. Ideally, one cathode is developed to satisfy the requirements of all of the systems, therefore, this strategy is employed. The mesoscale thrusters generate the most hostile plasma environments because of their densities, therefore cathodes will be developed for (Regime I) and tested in these environments first. The challenge at hand is to provide 50-200 $mA/cm^2$ for more than 6000 hours with approximately 35 V at no more than 10 mW/mA (not including the power consumed coupling to the ion beams).

The FE cathode technology which has demonstrated the highest current density, lowest operating voltages, and highest efficiency to-date is the Spindt-type field emitter array (FEA) cathode. It is also the most mature and accessible of the microfabricated FE cathodes. Less mature FE cathode technologies include thin Negative Electron Affinity (NEA) films and carbon nanotubes. Rigid carbon nanotube cathodes have not yet been grown in microfabricated gate structures, therefore the operating voltages have been greater than 100 V with efficiencies much lower than 10 mW/mA. Carbon and diamond NEA films have demonstrated turn-on electric fields which are lower than the Spindt-type cathodes and 100 $mA/cm^2$, however, either their operating voltages are too high or their efficiencies are too low [23,24,8]. Spindt-type cathodes have demonstrated current densities greater than 2000 $A/cm^2$ from Mo [25,26] arrays and 2 $A/cm^2$ from Si arrays [27] in UHV in triode configurations with efficiencies higher than 0.01 mW/mA and lifetimes greater than 8000 hours.

At this time it is believed that to meet the current density and lifetime requirements of the EP applications, the Spindt-type cathodes should be coupled with carbide or NEA material films. Experiments have shown that xenon will not affect the work function of Mo, Si, and C cathodes. [28] It has also been shown that the energy threshold for sputtering Mo and Si FEA cathodes with xenon ions is 49 eV and 63.7 eV, respectively [28]. The self-generated ions consist of both single and double ions if the cathode is operated above 35-37 V. At operating voltages below ~85 V, the cathode erosion process is dominated by the double ions. Mo and Si FEA cathode operating voltages will then be limited to ~37 V, approximately the double ion ionization potential of xenon, to achieve lifetimes greater than 6000 hours in a xenon environment where only the self-generated ion population is considered [28]. In the thruster environment, the charge-exchange ion population will further limit the operating voltages. This population of ions also consists of both doubly and singly charged ions. With operating voltages no higher than 37 V, the erosion process is again dominated by the double ions. This ion population will further limit the operating voltages to approximately 5 V (Mo) and 13 V (Si) because ions will be accelerated through approximately 20 V before entering the gate electrode apertures [28]. With optimistic FEA cathode characteristics including gate aperture radii of 0.2 μm, excellent uniformity, effective tip radii of 4 nm [29], and packing densities of $5x10^7$ $tips/cm^2$, modeling results show that it is impossible to attain 100 $mA/cm^2$ with Mo and Si FEA cathodes operating in the plasma environment generated by a Hall or ion thruster [28]. Other cathode configurations limitations include a lower limit on cathode gate electrode thickness because of potential delamination due to excessive heating from electron current and ion bombardment in a plasma environment. The performance can be improved by coating the cathodes with a lower work function material; it is anticipated that ~3.5 eV will be required. If the coating decreases the sputter yield also, higher operating voltages may be tolerated while meeting the EP system lifetime requirements. Materials with these properties could include HfC [30] ZrC [31], and carbon [23]. Mo and Si FEA cathodes have been successfully coated with carbide and carbon films [32,33,34,35,36]. These films have significantly improved the cathode performance in current and stability in UHV and

in more hostile environments. The cathode materials must also demonstrate stability in ground test facilities where the oxygen partial pressure could be ~$10^{-7}$ Torr. Some temporary performance degradation from limited oxygen adsorption is tolerable if it is reversible and can be temporarily compensated by additional cathodes at little cost. Depending on the performance of the FEA cathodes with the thin film coatings, the cathode performance with these films may still not meet both the current density and lifetime requirements.

Further cathode ruggedization is recommended with an electrostatic ion filter and an arc protection architecture. An ion filter should be used to retard the flow of charge-exchange or discharge ions to the cathode microtips. Without this flux of ions, the tolerable operating voltages will increase by more than 20 V and the current by several orders of magnitude while satisfying the lifetime requirements. A current limiting architecture that electrically isolates segments of an array of tips will also extend cathode lifetime. In the hostile thruster environments the cathodes will be contaminated by cathode, thruster propellant, and facility materials. In space, micrometeroids could impact the cathode and short out tips and gates. Often this contamination results in excessively high current densities and arcing between the tips and the gate electrode. Several architectures have been recommended to limit the current through a tip to prevent arc formation. One appealing current limiting configuration is the VErtical Current Limiting (VECTL) architecture [37] because it is a passive configuration which is microfabricated with the cathode. Packing densities of $5x10^7$ tips/cm$^2$ have been achieved with this architecture. Stable-resistivity wafers on the Si substrates could further stabilize the cathode performance. The field effect transistor configuration is another current limiting architecture option; however, this configuration could significantly reduce the packing density of the arrays of microtips. A segmented array with fuse interconnects has also been suggested to isolate damaged array segments from the larger integrated array. [38]

## FEA CATHODE TESTING IN ELECTRIC PROPULSION SYSTEM ENVIRONMENTS

The results from testing in electric propulsion system environments and in simulated environments are discussed in this section. Some results from cathode testing in xenon environments representative of ion and Hall thruster environments and oxygen environments representative of electrodynamic tether environments are presented. Details from a Mo FEA test with an In-FEEP are also discussed.

### Mo and ZrC/Mo FEA Cathode Behavior in Xenon Environments

Mo and ZrC/Mo cathodes have been tested in similar environments to compare their performance responses. A performance comparison is shown in Figure 3. The only difference between the cathodes is the 10-20 nm ZrC film on one of the cathodes. The Mo array is from SRI International and the coating was deposited at Aptech Inc. These results show that the ZrC/Mo cathode is more stable than the Mo cathode in a primarily xenon environment. The xenon pressure during these experiments was approximately $10^{-6}$ Torr, while the oxygen partial pressure was approximately $10^{-8}$ Torr. The operating voltages were approximately the same at 36-37 V. The current degradation observed was reversible; the cathode performance recovered during operation in ~$10^{-9}$ Torr. The results of this experiment proved that operating at such low voltages would enable operation of these cathodes in simulated ion and Hall thruster xenon environments.

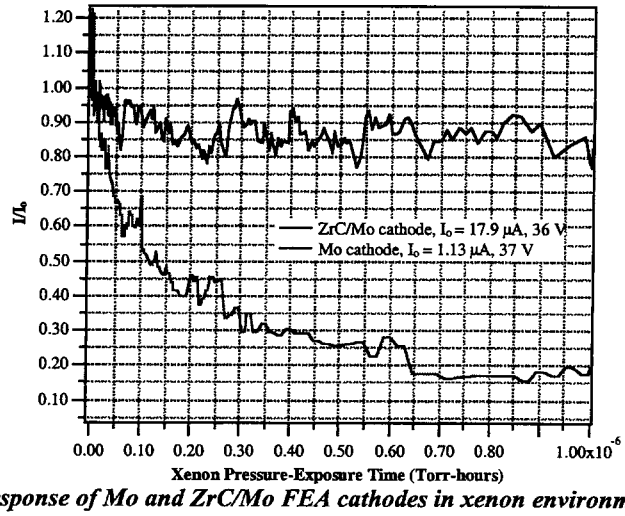


***Figure 3. Performance response of Mo and ZrC/Mo FEA cathodes in xenon environments.***

During one long duration exposure experiment to primarily a xenon environment, sputtering damage resulted in performance degradation. The cathode current significantly decayed, the gate current signifcantly increased and the performance showed signs of discharging. After the exposure experiment, the cathode performance slowly decayed every time it was operated. The cathode performance would recover slightly while it was not operating. With speculation that an oxide film had formed that would charge up during operation and disharge while it was off, the cathode current was significantly increased to try to improve the electron stimulated desorption of the oxide. The results of this experiment are shown in Figure 4. Instead of cathode self-cleaning, the results suggest that the surface film charged up more quickly and discharged itself through the gate electrode. Figure 4 shows the gate current, anode current and tip current. Gate current spikes, which could be small discharges, cause gate voltage drops because of the 1 M-Ohm resistors between the gate electrode and the power supply. The gate voltage during this experiment was ~85 V.

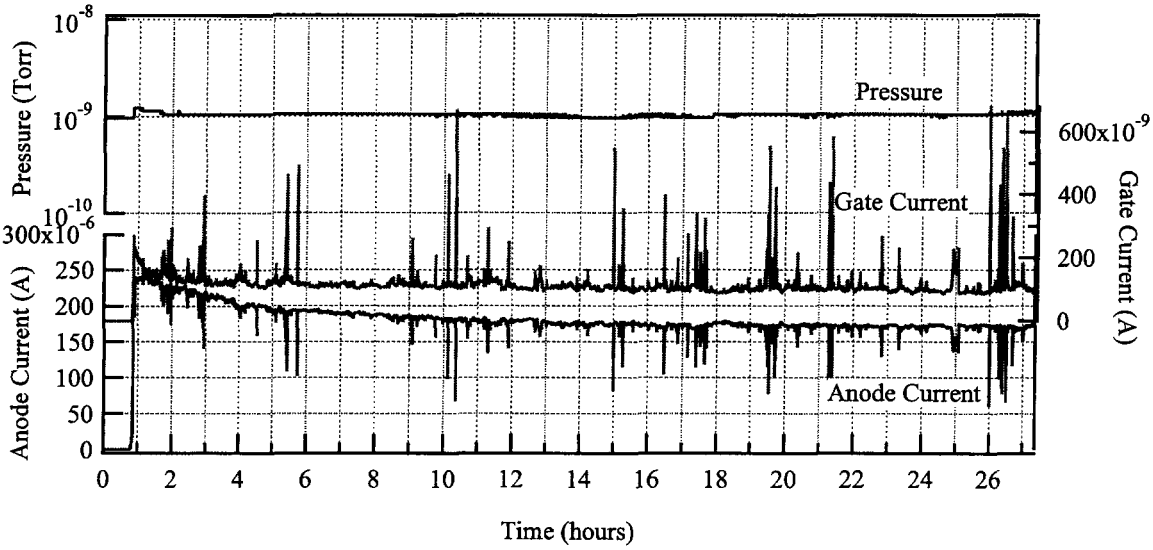


***Figure 4. Performance response of Mo and ZrC/Mo FEA cathodes in xenon environments.***

**FEA Cathode Behavior in Oxygen Environments**

Mo and ZrC-caoted Mo FEA cathodes both exhibit similar performance decay rates in oxygen environments. The results of some of these experiments are shown in Figure 5. These experiments were conducted at different pressures, different currents, different operating voltages and with different cathodes. The results are remarkably similar and repeatable. Figure 6 shows the decay of a Mo FEA cathode operating in an oxygen environment. The objective of this experiment was to show that the cathode current would eventually stabilize. After 6 hours at $10^{-6}$ Torr, the current continued to decay beyond a current decrease by two orders of magnitude. With attempts made to stabilize the current by increasing the voltage, the current decay rate only increased. There seemed to be a significant increase in the decay rate when the gate voltage exceeded 60 V.

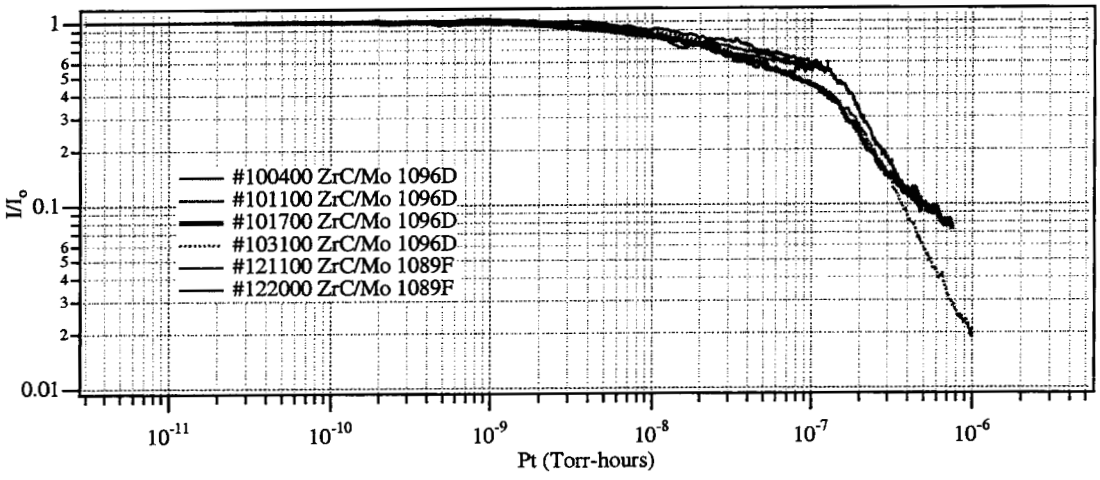


*Figure 5. Performance response of Mo and ZrC/Mo cathodes in oxygen environments.*

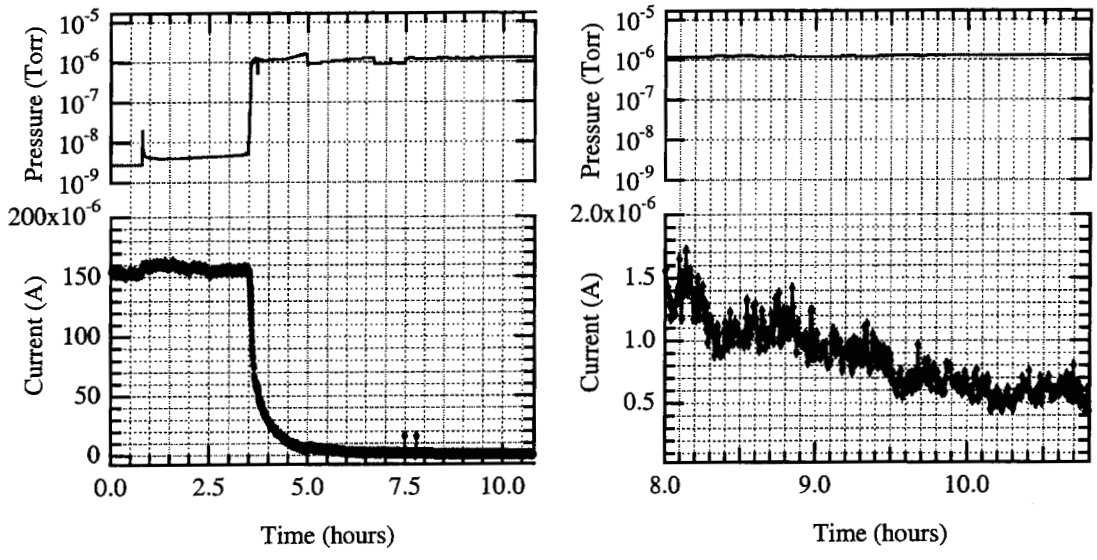


*Figure 6. Performance of Mo FEA cathode in oxygen environment showing continuous performance degradation.*

**FEA Cathode Behavior in FEEP Environment**

A Mo Spindt-type cathode from SRI International was used to demonstrate that a FEA cathode can be used to neutralize the charge of an In-FEEP from the Austrian Research Center Seibersdorf (ARCS). [39] The environment during these missions was not favorable for Spindt-type field emission cathode operation. While the chamber was UHV compatible, the cathode was susceptible to contamination by the partial pressures of oxygen in $10^{-7}$-$10^{-6}$ Torr of air and back sputtered indium and aluminum from the ion beam target and emissive probe which were positioned only 1-6 cm from the ion and electron sources. The cathode successfully demonstrated that it could be used to neutralize the thruster charge with remarkable stability while operating at 66 μA and 52 V for approximately 30 min. The cathode current actually increased by 2 μA during this period. This cathode consisted of 50,000 tips with 0.9 μm gate aperture diameters. Longer duration testing is required to further substantiate these results and cathode ruggedization will be required to achieve mission lifetime requirements of >6000 hours in the spacecraft environment. The In-FEEP and FEA cathode tested together are shown in Figure 7.

Figure 7. A FEA Cathode and In-FEEP.

## FEA CATHODE MATERIALS SELECTION

It has been shown that conventional Spindt-type cathode materials are not compatible with oxygen environments; therefore, suitable materials must be identified which also have the material characteristics required for field emitter cathodes. These properties include a low and stable work function and good conductivity in oxygen-rich environments. The tolerable work function depends on the gate aperture diameter, tip emission uniformity ($\Delta s$), tip packing density, and operating voltage limitations. A cathode in equilibrium with its environment should maintain a work function no higher than 4.8 eV if gate voltages as high as 90 V are tolerable. If lower operating voltages are necessary, lower work function materials will be required. For example, experimental results suggest that the operating voltage limitation is between 60 and 70 V for ZrC-coated Mo cathodes operating in oxygen environments. If the equilibrium work function of ZrC in oxygen environments is 4.4 eV (change in work function estimated from exposure experiments after $8.9 \times 10^{-6}$ Torr-hours), then required operating voltages will be between 40 and 80 V depending on the emission uniformity quantified by $\Delta s$ and the cathode feature sizes. However, after this exposure, the performance of the cathode continued to decay due to further changes in work function and/or surface conductivity. An attempt to compensate for the current decay by increasing the gate voltage actually lead to accelerated decay rates. This result may be due to tip sputtering and/or charging in the surface films during the exposures with the cathodes operating. Maintaining sufficient conductivity in an oxygen-rich environment and operating below the voltage threshold for sputtering are both critical in successfully integrating field emission cathodes with space-based applications.

The $\Delta s$ parameter for a cathode also significantly affects the cathode performance, but with a linear relationship. Variation in tip radius of curvature across the array is captured in the $\Delta s$ parameter. A smaller $\Delta s$ value is representative of a more uniformly emitting array of cones. The current cathode configuration has gate aperture radii of 4500 Å. $\Delta s$ values estimated from experiments performed on ZrC/Mo cathodes in this program were between 32 and 0.9 at <100 V (although values as low as 0.1 have been demonstrated at SRI International with Mo cathodes at much higher operating voltages, >100 V). With demonstrated $\Delta s$ values, lower work function materials with the aforementioned characteristics will be required to achieve 10 mA/cm$^2$ at the desired operating voltages of 30 V. Cathodes with smaller gate aperture diameters will demonstrate lower $\Delta s$ values at such low voltages to further improve cathode performance.

Changes in surface film conductivity will also affect the tolerable work function limit and negatively affect the cathode performance. Some materials oxidize quickly in an atomic oxygen environment with a thickness limited only by the thickness of the base material as believed to be the case with Mo. An oxide film on the tips can increase or decrease the work function significantly. An oxygen film on the surface typically increases the work function. Perhaps most importantly, as noted above, an oxide film will reduce the surface conductivity which results in charging up of the film leading to further current degradation [Shaw, 2000]. Both responses to the oxygen environment will negatively affect the performance of the cathode by decreasing its stability and increasing its operating voltages to regimes that could significantly decrease the cathode lifetime. Therefore, some materials which will form conductive oxides in oxygen-rich environments have been identified as cathode material candidates. The required conductivity for the surface films is uncertain, but most likely depends on the film thickness.

Table 3. Cathode current densities for various operating voltages, $V_g$, work functions, $\phi$, packing densities, pd, tip radii, $r_t$, spread in tip radii, $\Delta s$, gate aperture radii, $r_g$, tip half cone angle, $\beta_c$.

| pd (tips/cm$^2$) | $\beta_c$ | $r_t$ | $\Delta s$ | $r_g$ | $\phi$ | $V_g$ | J (mA/cm$^2$) |
|---|---|---|---|---|---|---|---|
| $10^7$ | 0.26 | 40 | 2 | 4500 | 3.8 | 35 | 0.2 |
| $10^7$ | 0.26 | 40 | 2 | 4500 | 3.8 | 40 | 2.6 |
| $10^7$ | 0.26 | 40 | 2 | 4500 | 3.8 | 50 | 89 |
| $10^7$ | 0.26 | 40 | 2 | 4500 | 4.1 | 50 | 15.4 |
| $10^7$ | 0.26 | 40 | 100 | 4500 | 4.1 | 60 | 4.6 |
| $10^7$ | 0.26 | 40 | 100 | 4500 | 4.1 | 70 | 30.0 |
| $10^7$ | 0.26 | 40 | 500 | 4500 | 4.1 | 70 | 7.6 |

| | | | | | | | |
|---|---|---|---|---|---|---|---|
| $10^7$ | 0.26 | 40 | 2 | 2000 | 3.8 | 35 | 9.3 |
| $10^7$ | 0.26 | 40 | 2 | 2000 | 4.1 | 40 | 12.5 |
| $10^7$ | 0.26 | 40 | 10 | 2000 | 4.1 | 40 | 2.5 |
| $10^7$ | 0.26 | 40 | 10 | 2000 | 4.1 | 50 | 68.0 |
| $10^7$ | 0.26 | 40 | 100 | 2000 | 4.1 | 40 | 0.2 |
| $10^7$ | 0.26 | 40 | 100 | 2000 | 4.1 | 50 | 6.8 |
| $10^7$ | 0.26 | 40 | 500 | 2000 | 4.1 | 60 | 14.0 |
| $10^7$ | 0.26 | 50 | 500 | 2000 | 4.1 | 40 | 0.006 |
| $10^7$ | 0.26 | 40 | 2 | 4500 | 3.8 | 60 | 1.08 |
| $10^7$ | 0.26 | 40 | 2 | 4500 | 4.4 | 60 | 49.0 |
| $10^7$ | 0.26 | 40 | 2 | 4500 | 4.6 | 60 | 17.0 |
| $10^7$ | 0.26 | 40 | 2 | 4500 | 4.7 | 60 | 10.4 |

Several materials have been identified in this investigation as promising candidates for the tether application. They have been chosen because of their excellent work functions and anticipated superior resistance to oxidation and/or the anticipated formation of conductive oxides in oxygen-rich environments. These materials include Mg on Pt (Pt/Mg), NbC on Nb (Nb/NbC), NbNi on Nb (Nb/NbNi), C on Pt (Pt/C), MgPt on Pt (Pt/MgPt), and Ru on Ta (Ta/Ru). Mo and ZrC on Mo (Mo/ZrC) are also being included in the investigation for comparison. Pt/Mg was selected because it forms a conductive oxide with an excellent work function. Thin MgO surface films on field emission cathodes have demonstrated acceptable conductivity. The work function of MgO has been measured to be 3.1-4.4 eV [Tsarev, 1955], and the measured work function of Pt is 5.32 eV [Femenko, 1966], however, the work function of MgO on Pt has been measured to be 3.19 [Jentzsch, 1908] and 3.31 eV [Spanner, 1924]. Since intermetallic films can be more stable in oxidizing environments Pt/Mg and Pt/MgPt film combinations are both under investigation. There are concerns about observed electron-induced oxygen desorption from the MgO on the cathode surface affecting the cathode stability. This process could expose Mg which could be easily sputter removed and cause increases in cathode work function and tip radii. The oxygen environment could sufficiently replenish the desorbed oxygen before this process occurs. Nb/NbC was selected because of its excellent work function, a developed Spindt-type field emission cathode fabrication process, and some promising results recently released [Mackie, et al., 2001]. NbC cones have been deposited into 0.4 um diameter gate apertures with excellent results. The cathode performance was not affected by operating in ~$5x10^{-7}$ Torr of oxygen for 40 min. Nb/NbNi was selected because of fabrication experience, anticipated stability in oxidizing environments, decent work function, and good NiO conductivity. It is anticipated that the intermetallic films will offer a higher resistance to oxidation than the film constituents. Ru and Ta film combinations were selected because of the work function and conductivities of the materials and their oxides. Silicon FEA cathode tips with Ta and then Ru films deposited on them were oxidized with excellent results. [Yoon et al., 2000] The $RuO_2$ surface oxide was conductive and the work function was identical to the work function of Ta, 4.1 eV. The $RuO_2$-Ta interface was incredibly stable, prohibiting oxidation of the Ta base film.

**Oxygen Ion Penetration Depth into Material** SRIM (Stopping and Range of Ions into Matter) [Ziegler et al. 1985] was used to approximate the ion penetration depth in various cathode candidate materials. SRIM consists of a group of programs which are used to determine the stopping range of ions into matter using a full quantum mechanical treatment of collisions between ions impinging on a target and the atoms in that target. Chemical reactions with the target are not considered. The results of the calculations with SRIM are presented in Table 4.

**Material Sputter Yield for Oxygen Ions** TRIM (Transport of Ions in Matter) was used to estimate and compare the sputter yields of various cathode candidate materials. TRIM can be used to determine the final 3-D distribution of the ions and also all kinetic phenomena associated with the ion's energy loss: target damage, sputtering, ionization, and phonon production. It is not capable of considering the effects of chemical reactions between the ions and target material on the sputter yield. 500 ions were bombarded the targets to obtain the statistics for the sputter yield estimates. The results of the calculations with SRIM are presented in Table 4. The calculated sputter yields are compared for many of the cathode candidate materials.

Table 4. Material penetration depth, d, and sputter yield, Y, for atomic oxygen ions with the energies identified and targets with the materials and densities identified.

| Material (t(nm)) | Density ($g/cm^3$) | d (nm) 50 eV | d (nm) 100 eV | d (nm) 200 eV | Y (atoms/ion) 100 eV |
|---|---|---|---|---|---|
| Ir | 2.24 | 0.3 | 0.4 | 0.5 | 0.020 |
| Mg | 1.73 | 0.9 | 1.3 | 1.9 | 0.584 |
| Mo | 10.20 | 0.4 | 0.5 | 0.7 | 0.136 |
| Nb (10) | 8.57 | 0.4 | 0.6 | 0.8 | 0.120 |
| NbC (10) | 7.60 | | 0.7 | | 0.050 (Nb) 0.044 (C) |

| | | | | | |
|---|---|---|---|---|---|
| Pt | 2.14 | 0.3 | 0.4 | 0.6 | 0.022 |
| Ru (10) | 1.23 | 0.3 | 0.4 | 0.6 | 0.148 |
| Ta | 1.66 | 0.4 | 0.5 | 0.7 | 0.014 |
| Zr (10) | 6.49 | 0.5 | 0.8 | 1.1 | 0.128 |
| ZrC | 6.73 | 0.5 | 0.6 | 0.8 | 0.054 (Zr)<br>0.038 (C) |

**Sample Preparation-Film Deposition** The films under investigation were deposited at Aptech Inc. on 0.5 mm-thick silicon wafers. Si wafers were sputter cleaned by a 260 V Ar ion beam for 5 minutes before the films were deposited on the substrates. Ti films were deposited on the Si wafers before film deposition to improve adhesion. Ti film thickness was 10 nm. ZrC was evaporated from zone refined single crystal onto Mo for the ZrC/Mo sample. NbNi was evaporated from a NbNi alloy target onto the Nb film for the NbNi/Nb sample. Mg and Pt were co-deposited onto the Pt film for the MgPt/Pt sample. Ru and Ta were co-deposited onto the Ta film for the RuTa/Ta sample. A slightly higher concentration of Ru is expected in the surface film. The thickness of the films on the samples are given in Table 3.

**Sample Exposures to Atomic Oxygen**

The material samples were exposed to ozone environments to simulate a dose of atomic oxygen to the cathodes similar to the dose that they will experience in a LEO environment. An UltraViolet Ozone Cleaning System (UVOCS) was used in these exposures. A new lamp in this system produces 60-100 ppm of ozone. It is estimated that this lamp has been used for <1000 hours. The lamp intensity typically decays by 10 % in 1000 hours. Therefore, the ozone PPM in the source should range between 50 and 100 at atmospheric pressure. Ozone easily dissociates into molecular and atomic oxygen upon impacting the material surface providing a thermal flux of atomic oxygen to the samples. The lowest PPM of ozone approximated for this system is 50. Assuming temperatures in the ozone source are approximately 300K, the flux of ozone to the samples is ~$4x10^{22}/m^2/s$. In LEO ambient at 300 km, the flux of atomic oxygen to the cathodes would be$1.1x10^{17}/m^2/s$. A 30-day exposure would result in a total dose of $2.8x10^{23}/m^2$. A 1-month exposure to the LEO environment could be accomplished with a 7-second exposure to ozone in the ozone source used. The samples were exposed to ozone for 5 and 20 minutes to determine if the films would passivate themselves after such long exposures, if the oxide films formed were stable, and how the extreme exposures would affect the cathode material properties.

**AES-Argon Ion Sputter Depth Profiling**

Surface oxide thickness on the films was characterized both before and after the films were exposed to atomic oxygen environments. The native oxide film thickness was determined in addition to the surface oxide thickness after exposure to ozone for 5 and 20 minutes. Depth profiling was conducted using a PHI 660 Scanning Auger Microprobe equipped with a single pass cylindrical mirror analyzer and PHI **04-303** differentially pumped sputter ion gun. Auger electron spectra were acquired at a chamber pressure of approximately $10^{-8}$ Torr with a 3 keV electron beam. The energy of the argon ions sputtering the films was 2 keV and current was 25 mA with a 2x2 mm raster. The ions bombarded the samples at 60° from the surface normal. The Auger spectra acquired represents, on average, the composition of the top 1 nm of the surface, but can detect electrons from as deep as 10 nm below the surface.

The films were sputtered at various time steps separated by Auger spectra measurements to produce plots of the variation in surface species in time, which can be converted to depth with the material sputtering rate. The sputtering rate of the thin film alloys was estimated employing the assumption that the surface film has been removed when the substrate signal reaches 50% of its final intensity. It is then assumed that the oxide film is removed with the same sputter rate to approximate the thickness of the surface oxide. The surface oxide thickness is approximated by the material sputter rate and time required for the oxygen signal intensity to drop to 50% of its original value. The results of the depth profiling are shown in the following several figures. Table 4 presents the calculated thickness of the surface oxides for the material combinations investigated.

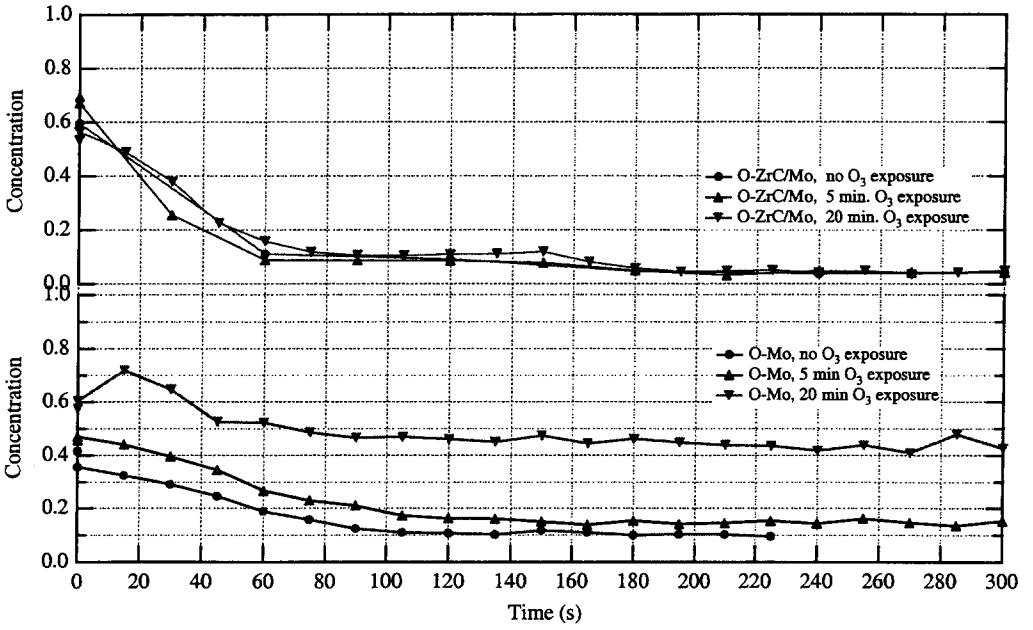


Figure 1. Oxygen concentrations for Mo and ZrC/Mo films.

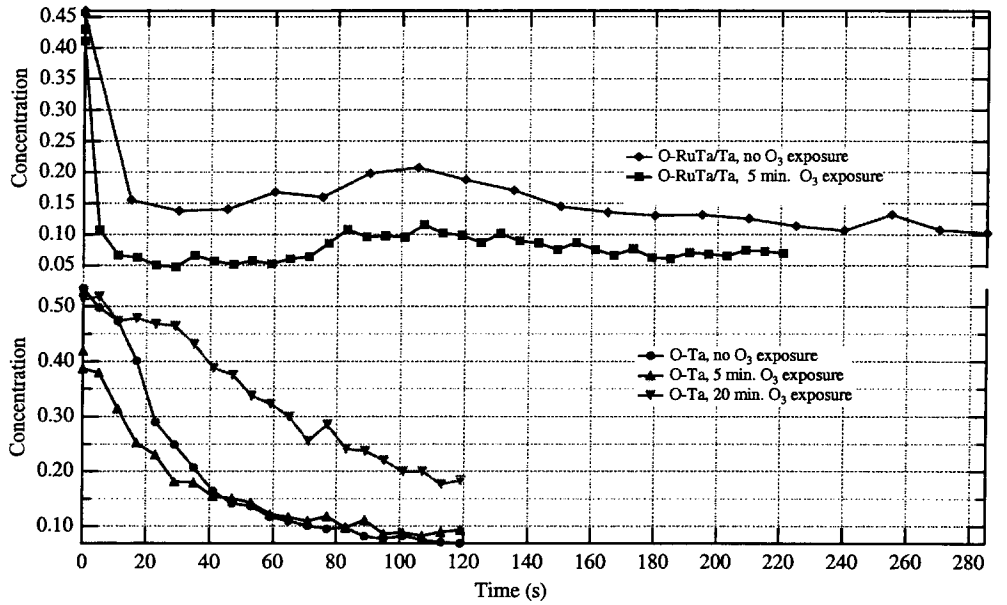


Figure 2. Surface component concentrations for Ta and RuTa/Ta films.

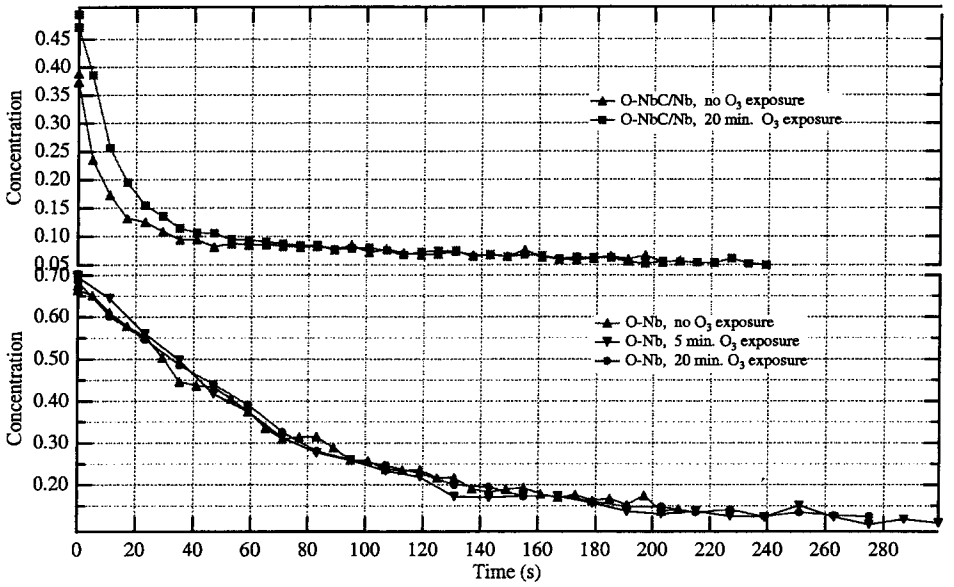


Figure 3. Oxygen concentrations for Nb and NbC/Nb films.

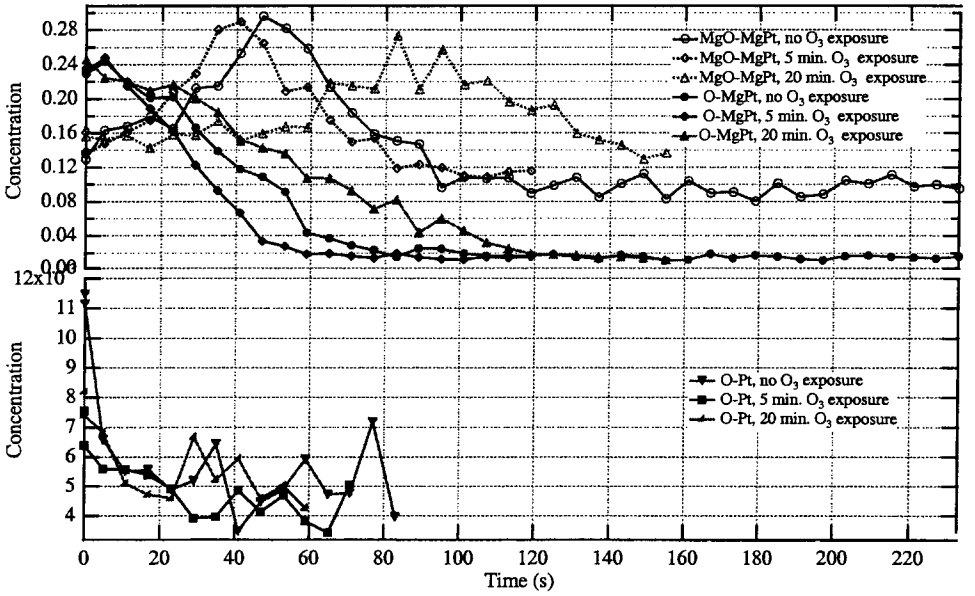


Figure 4. Surface concentrations for Pt and MgPt films

***Table ##. Comparison of the resistance and work function responses to a 20 exposure to atomic oxygen.***

| Sample Identity | Surface Film | Thickness (nm) | Base film | Thickness (nm) | Initial $\Phi_w$ (eV) | Final $\Phi_w$ (eV) | Initial R (mOhms) | Final R (mOhms) | Oxide Thickness (nm) |
|---|---|---|---|---|---|---|---|---|---|
| **Ideal** | | | | | | **<4.8** | | **<74** | |
| MgPt | | | MgPt | 200 | 4.1 | 4.38 | 30 | 30 | |
| Mo | | | Mo | 300 | 4.6 | | 74 | ?? | |
| Nb | | | Nb | 300 | 4.25-4.6 | | 74 | ?? | |
| NbC/Nb | NbC | 10 | Nb | 500 | 4.32-4.65 | 4.41 | 43 | ?? | |
| NbNi/Nb | NbNi | 10 | Nb | 300 | 4.3-4.49 | 4.51 | 50 | 45 | |

| | | | | | | | | | |
|---|---|---|---|---|---|---|---|---|---|
| Pt | | | Pt | 200 | 4.82 | 5.13 | 47 | 45 | |
| PtC/Pt | PtC | 10 | Pt | 200 | 4.05-4.57 | 4.79 | 26 | ?? | |
| Ru/Ta | Ru | 10 | Ta | 300 | 4.0-4.85 | 4.78 | 54 | ?? | |
| RuTa/Ta | RuTa | 10 | Ta | 300 | | 4.41 | 114 | 127 | |
| Ta | | | Ta | 300 | 4.0-4.1 | 4.16 | 261 | 265 | |
| ZrC/Mo | ZrC | 10 | Mo | 300 | 3.65-4.5 | 4.91 | 176 | 173 | |

## CONCLUSIONS

The results presented in this paper represent a program in progress. Many challenges have been identified. Some modeled solutions have been demonstrated. Robust cathode architectures to survive arcing and debris impact events must be fabricated. FEA cathodes with smaller gate apertures and larger packing densities are being fabricated to respond to the current density and operating voltage objectives and limitations. In the search for the FEA cathode materials required for compatibility with electric propulsion applications, progress has been made. The results presented encourage the fabrication of NbC./Nb, NbNi/Nb and MgPt FEA cathodes. There are still other materials including IrO2, that have been identified by others as having very promising characteristics for oxygen-rich environments. Several other conductive oxides will also be considered for these applications.

## ACKNOWLEDGEMENTS

The authors would also like to gratefully acknowledge NASA MSFC (John Cole, Dr. Kai Hwang, Randy Bagget, Les Johnson) and Tethers Unlimited Inc. (Dr. Rob Hoyt) for funding the development of field emission cathodes for space-based applications and Drs. Capp Spindt, Babu Chalamala and Paul McClelland for their valuable advice on field emission cathode operation and materials. The research described in this paper was carried out at the Jet Propulsion Laboratory, California Institute of Technology, under a contract with the National Aeronautics and Space Administration

[1] Gamero-Castano, M., Hruby, V., "Characterization of a Colloid Thruster Performing in the micro-Newton Thrust Range," IEPC-01-282.

[2] Sohl, G., Fosnight, VV., Goldner, SJ., Speiser, RC. Cesium Electron Bombardment Ion Microthrustors. In: 5th Aerospace Sciences Meeting. 1967. Paper No. AIAA-67-81.

[3] Gorshkov, O., Muravlev, VA., Grigoryan, VG., Minakov, VI. Research in Low-Power ion Thrusters with Slit-Tye Grid Systems. In: 35rd AIAA/ASME/SAE/ASEE Joint Propulsion Conference and Exhibit. 1999. Paper No. AIAA-99-2855.

[4] Mueller, J., Pyle, D., Chakraborty, I. Ruiz, R., Tang, W., Lawton, R. Microfabricated Ion Accelerator Grid Design Issues: Electric Breakdown Characteristics of Silicon Dioxide Insulator Material. In: 34th Joint Propulsion Conference and Exhibit, 1998. Paper No. AIAA-98-3923.

[5] Khayms, V., Martinez-Sanchez, M. A 50 W Hall Thruster for Microsatellites. Accepted for publication in AIAA Progress Series on Micropropulsion, planned for release in July 2000.

[6] Belikov, M.B., Gorshkov, OA., Rizakhanov, RN., Shagayda, AA., Khartov, SA. Hall-Type Low- and Mean Power Thrusters Output Parameters. In: 35th AIAA/ASMA/SAE/ASEE Joint Propulsion Conference and Exhibit. 1999. Paper No. AIAA-99-2571.

[7] Colbert, TS., Gavryushin, VM., Khartov, SA., Kim, V., Popov, GA., Tchuyan, RK. Perspecitves of Small SPT Development and Application.

[8] Marrese, CM. Compatibility of Field Emission Cathode and Electric Propulsion Technologies. Ph.D. Dissertation, University of Michigan. 1999.

[9] Wang, J., Brinza, DE., Young, DT., Nordholt, JE., Polk, JE., Henry, MD., Goldstein, R., Hanley, JJ., Lawrence, DJ., Shappirio, M. Deep Space One Investigations of Ion Propulsion Plasma Environment. Accepted for publication in J. Spacecraft & Rockets, 2000.

[10] Taylor, G., Disintegration of Water Drops in an Electric Field. Proceed. of the Royal Society 1964;A 280:383-97.

[11] Fehringer, M., Rudenauer, Steiger, W. Space-Proven Indium Liquid Metal Field Ion Emitters for Ion Microthruster Applications. In: 33rd AIAA/ASME/SAE/ASEE Joint Propulsion Conference and Exhibit. 1997. Paper No. AIAA-97-3057.

[12] **Marcuccio, S., Gianneli, S., Andrenucci, M. Attitude and Orbit Control of Small Satellites and Constellations with FEEP Thrusters. In: 25th International Electric Propulsion Conference. 1997. Paper No. IEPC-97-188.-juergen's reference.**

[13] Spindt, CA. An Efficient Low-Voltage Field Ion Source, In: 1st Int. Vacuum Microelectronics Conf. 1988.

[14] Mitterauer, J., Miniaturized Liquid Metal Ion Sources (MILMIS). IEEE Trans. Plasma Sci., 1991:19(5)790-9.

[15] Perel, J., Bates. T., Mahoney, J., Moore, RD., Yihiku, AY., Research on Charged Particle Bipolar Thrustor. AIAA Paper 67-728, Colorado Springs, CO, Sept. 1967.

[16] Hubberman, MN., Rosen, SG., Advanced High-Thrust Colloid Sources. J. Spacecraft 1974;11(7):475-80.
[17] De La Mora, JF. The Effect of Charge Emission from Electrified Liquid Cones. J. Fluid Mech. 1992;243:561-74.
[18] Jahn, R.G. Physics of Electric Propulsion. McGraw-Hill, 1968.
[19] Huberman, MN., Rosen, SG. Advanced High-Thrust Colloid Sources. J. Spacecraft, 1974:11(7):475-480.
20 Paine, M. and Gabriel, S., A Micro-Fabricated Colloidal Thruster Array, In: 37th AIAA/ASMA/SAE/ASEE Joint Propulsion Conference and Exhibit. 2001. Paper No. AIAA 2001-3329.
[21] This value was calculated from the assumptions that the discharge chamber pressure is $10^{-4}$ Torr at 300 K and 10 % ionization fraction. The ion current density was calculated assuming an ion temperature of 2 eV and Bohm velocity with $J_i=0.6en_iv_{bohm}$.
[22] **Joe and my book chapter**
[23] Geis, MW., Twichell, JC., Lyszarz, TM. Diamond Emitters Fabrication and Theory. J. Vac. Sci. Tech. B. 1996:14(3):595-8.
[24] Tolt, ZL., Fink, RL., Yaniv, A. Electron Emission from Patterned Flat Cathodes. J. Vac. Sci. Technol. B 1998;16(3):1197-1198.
[25] Murphy, RA., Harris, CT., Matthews, RH., Graves, CA., Hollis, MA., Kodis, MA., Shaw, J., Garven, M., Ngo, MT., Jensen, KL., IEEE International Conference on Plasma Science, San Diego, CA, May 19-22, 1997.
[26] Spindt, C. A., Brodie, I., Technical Digest of the 1996 IEEE International Electron Devices Meeting (IEDM), 12.1.1 (1996); CA. Spindt, CE. Holland, PR. Schwoebel, I. Brodie, IEEE International Conference on Plasma Science, San Diego, CA, May 19-22, 1997.
[27] Temple, D., Palmer, WD., Yadon, LN., Mancusi, JE., Vallenga, D., McGuire, GE. Silicon Field Emitter Cathodes: Fabrication, Performance, and Applications. J. Vac. Sci. Technol. A. 1998;16(3): .
[28] Marrese, CM., Polk, JE., Jensen, KL., Gallimore, AD. , Spindt, C. , Fink, RL., Palmer, WD. An Investigation into the Compatibility of Field Emission Cathode and Electric Thruster Technologies: Theoretical and Experimental Performance Evaluations and Requirements, *Micropropulsion for Small Spacecraft*, AIAA Progess Series Vol. 187, edited by M. Micci and A. Ketsdever, AIAA , Reston, VA, 2000, Chapter 11.
[29] Jensen, KL. Field Emitter Arrays for Plasma and Microwave Source Applications. Physics of Plasmas 1999;6(5):2241-53.
[30] Mackie, WA., Morrissey, JL., Hindrichs, CH., Davis, PR. Field Emission from Hafnuim Carbide. J.Vac. Sci. Technol. A 1992;10(4): 2852-6.
[31] Mackie, WA., Hartman, RL., Anderson, MA., Davis, PR. Transition Metal Carbides for Use as Field Emission Cathodes. J. Vac. Sci. Technol. B 1994;12(2):722-6.
[32] Xie, T., Mackie, WA., Davis, PR. Field Emission from ZrC Films on Si and Mo Single Emitters and Emitter Arrays. J. Vac. Sci. Technol. B 1996;14(3):2090-2.
[33] Mackie, WA., Xie, T., Matthews, MR., Routh, BP. Jr., Davis, PR. Field Emission from ZrC and HfC Films on Mo Emitters. J. Vac. Sci. Technol. B 1999;17(2): 2057-62.
[34] Rakhshandehroo, MR. Design, Fabrication, and Characterization of Self-aligned Gated Field Emission Devices. Ph.D Dissertation, The University of Michigan. 1998. Tech. rep. no. SSEL-284.
[35] Lee, S., Lee, S., Lee, S., Jeon, D., Lee, KR. Self-Aligned Silicon Tips with Diamond-like Carbon. J. Vac. Sci. Technol. B 1997;2:457-9.
[36] Jung, JH., Ju, BK., Lee, YH., Jang, J., Oh., MH. Emission Stability of a Diamond-like Carbon Coated Metal-tip Field Emitter Array. J. Vac. Sci. Technol. B 1999;17(2):486-8.
[37] Takemura, H., Tomihari, Y., Furutake, N., Matsuno, F., Yoshiki, M., Takada, N., Okamoto, A., Miyano, S. A Novel Vertical Current Limiter Fabricated with a Deep Trench Forming Technology for Highly Reliable Field Emitter Arrays. Tech. Digest IEEE-IEDM, 1997;709.
[38] **SRI Int. reference on fuse interconnects for large cathodes arrays.**
[39] IEPC FEEP Paper